12-2022

Development of an Electro-Centrifugal Spinning Setup for Nanofiber Production Research

David A. Treviño
The University of Texas Rio Grande Valley

DEVELOPMENT OF AN ELECTRO-CENTRIFUGAL SPINNING SETUP FOR NANOFIBER PRODUCTION RESEARCH

A Thesis

by

DAVID A. TREVINO

Submitted in Partial Fulfillment of the

Requirements for the Degree of

MASTER OF SCIENCE IN ENGINEERING

Major Subject: Mechanical Engineering

The University of Texas Rio Grande Valley

December 2022

DEVELOPMENT OF AN ELECTRO-CENTRIFUGAL SPINNING SETUP FOR NANOFIBER PRODUCTION RESEARCH

A Thesis
by
DAVID A. TREVINO

COMMITTEE MEMBERS

Dr. Arturo Fuentes
Co-Chair of Committee

Dr. Horacio Vasquez
Co-Chair of Committee

Dr. Mataz Alcoutlabi
Committee Member

December 2022

ABSTRACT

Trevino, David A., Development of an electro-centrifugal spinning setup for nanofiber production research. Master of Science in Engineering (MSE), December 2022, 55 pp., 3 tables, 24 figures, references, 17 Titles

Nanofiber production methods have been developed and improved over the course of decades. Each process allows for the creation of fibers with distinct properties that provide benefits to growing number of applications. On the same note, every process has shortcomings that keep them from being universally valid for all applications. This research considers electrospinning and centrifugal spinning systems and attempts to create a process which maintains high fiber qualities like small and consistent fiber diameters, and improved fiber alignment while providing a high fiber yield. The electro-centrifugal (EC) spinning machine that resulted was designed utilizing computer aided design (CAD) software to create crucial components and 3D print them with unique specifications that will help with vibration reduction, improved modularity, and facilitate cleaning procedure. When tested using 8 wt% polyethylene oxide (PEO) solution in deionized water (DI H2O), the machine was able to produce fibers at 2000, 3000 and 4000 rpm each run with a 0 V, 2000 V and 4000 V potential input. The produced fibers were measured using a scanning electron microscope (SEM) and ImageJ software. The tests showed that adjusting input voltage to higher values improved fiber quality and increased fiber yield. Increasing rotational velocity greatly increased fiber yield but increased fiber

diameters. The results showed promise for future testing procedures that could be fine-tuned to produce fibers within the nanometer range (1 – 100 nm).

DEDICATION

The completion of my master's studies would not have been possible without the love and support of my family. My mother, Yolanda Trevino, my father, Tomas Trevino, my mother-in-law, Gloria Saldana, and most importantly, my wife, Paula Trevino, and my two daughters, Clarissa and Vanessa, wholeheartedly inspired, motivated and supported me by all means to accomplish this degree. Thank you for all the love and patience.

ACKNOWLEDGMENTS

I will always be grateful to Dr. Arturo Fuentes and Dr. Horacio Vasquez, chairs of my thesis committee, for all their mentoring and advice in navigating through this everchanging road. Special thanks to Adriana Chapa and Carlos Delgado for all their assistance with setup and testing.

TABLE OF CONTENTS

LIST OF TABLES

Page

LIST OF FIGURES

Page

CHAPTER I

INTRODUCTION

Nanofibers and the methods behind their creation have been a topic of great interest in the past few decades (Yarin, 2001). The size constraints for a fiber to be classified as a nanofiber is a range between 1 – 100 nanometers in diameter. Attaining fibers of this size is a difficult task to achieve but doing so comes with an abundance of benefits. The fibers and fiber structures which can be created provide a great deal of benefits in various fields due to the high surface to volume ratio (Madani, 2013). The range of applications in which nanofibers can be utilized is constantly growing as production methods are developed, tested, and improved. Nanofiber production methods such as electrospinning and centrifugal spinning provide a baseline of processes that are adjusted to control the characteristics of the resultant fibers. Some of the most prominent fields that are benefiting from the use of nanofibers include drug delivery, apparel, fire protection technology, energy harvesting and storage, and cell regeneration, among others. To achieve the desired properties for each application, different production methods are used. These processes were developed through decades of research with varying parameters, materials, and unexpected byproducts which added favorable properties. Utilization of the right fiber production method is an integral part of attaining the characteristics necessary for each application. As different materials are tested, many new nanofiber production methods will emerge, and current methods can continue to improve for better production yield, wider range of viable material systems, and enhanced morphology/structure control.

1.1 Electrospinning

Nanofiber production methods and fiber material selection are heavily dependent on the application for which the nanofibers will be used. Methods to produce nanofibers are varied and have different sets of principles along with different strengths and weaknesses. Typically for the purpose of research and applications there are two particular nanofiber production methods which are most commonly seen. One of these methods is known as Electrospinning (schematic shown in Figure 1). In this process, a syringe with the solution to be processed is placed facing a collector which is charged with a negative voltage. The syringe is then charged with a positive voltage to the point where the charge within the droplet at the tip of the syringe becomes sufficiently strong to overcome the surface tension. This in turn creates the Taylor cone from which a jet of solution shoots out. Once the jet is traveling between the syringe and the collector, the voltage potential between the two electrodes causes the electrostatic forces which aid in stretching out the fibers until they finally land on the collector. (Rutledge, 2007) The resulting properties of this process and the low cost make electrospinning a very attractive option for fiber creation.

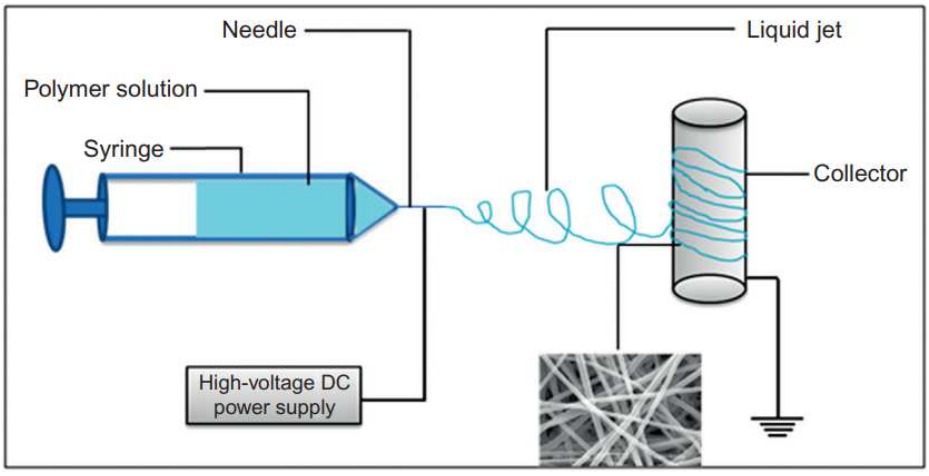

Figure 1: General laboratory electrospinning setup. (Unnithan, 2015)

Typically, a normal electrospinning setup is made up of three main components. These include a high-voltage power supply, a needle with a metallic tip, and a grounded collector as can be seen in figure 1. Varying parameters of the setups help in creating nanofibers with different properties. These changes can include things like changing the feed rate of the solution in the syringe, changing the distance between the collector and the syringe, using dynamic vs static collectors, and reorganizing the orientation of the collector to name a few. Using different solutions is another controllable parameter although it is limited. The solution utilized in an electrospinning setup does require the use of materials with a high enough dielectric constant which is needed to induce a reaction between the electrostatic forces and the solution. (Trevino, 2021) Although this is a limiting factor for electrospinning, materials systems that can be used have the ability to be fine-tuned to reach the desired characteristics once spun into nanofibers.

The controllable results which can be achieved make electrospinning a very useful method for the creation of nanofibers. Although highly adaptive, there are additional fiber production characteristics which limit electrospinning. One of the main issues is the low production rate when compared with alternative methods. Electrospinning setups normally operate at low feed rates for the syringe holding the solution. To put it into perspective, a typical electrospinning setup at standard feeding rates will produce about 0.1g/h, whereas Forcespinning™, a variant of centrifugal spinning, has been known to produce at rates higher than 1 g/min (Padron, 2013). The disparity between both processes helps show the opportunity to help advance the technology and seek alternative methods to alleviate the shortcomings of electrospinning.

1.2 Centrifugal Spinning

As previously mentioned, one of the main concerns for mass electrospinning nanofiber utilization is the low production rate. Many variants of the electrospinning process have been created to try to resolve this issue but although improvements are seen at times, the yield for these methods is still significantly low. A method that has gained popularity over the last few decades and helps supplement the low production rates is known as centrifugal spinning. This method makes use of centrifugal forces to produce solution into nanofibers. The solution is placed at the center of the system within a spinneret which spins on its z-axis. Metal collectors are placed radially surrounding the spinneret. Once initiated, the process creates fibers by rotating the spinneret at high velocities which causes the solution to extrude and stretch out as the solvent evaporates before being deposited on the collectors. The net yield that is typically seen in the centrifugal spinning process is significantly higher than that of alternative methods such as electrospinning at just a fraction of the time. Plus, the material systems which can be produced using this method are much diverse as it is able to produce fibers with low dielectric constants. However, just as electrospinning had the low net production drawback, centrifugal spinning methods have the disadvantage of producing fibers with inconsistent characteristics. Namely, varying fiber diameter and undesirable fiber alignment. Altering this method to allow maintaining its beneficial qualities while reducing or eliminating the undesirable ones could produce a method that can expand the possibilities of what nanofibers can be used for.

1.3 Material Selection and Poling

Manufacturing a system to produce nanofibers requires careful consideration to any potential enhancement or beneficiary characteristic that may result in the material. Paired with meeting the sought-out yields and ensuring the fiber qualities match the desired output, it is difficult to determine what one method might encapsulate everything necessary for the research

or application. One particular byproduct of electrospinning, for example, is a poling effect that is created in certain materials when produced using this method. The native piezoelectric properties of materials are enhanced when processed through the electrospinning method. The applied voltage helps alter the molecular alignment of the fibers. That paired with the naturally uniform alignment of the fibers that results from electrospinning all contribute to an increase in piezoelectric response in the produced fibers. These properties all make their respective methods very useful while still keeping them with their limiting factors. In order to achieve the best quality possible by combining two methods and taking advantage of both of the method's desirable qualities, a new process has to be created and tested. The fibers that result from this new process can be analyzed and compared to derivative versions of each individual method.

1.4 Hybrid Spinning

Overcoming the shortcomings typically seen in conventional nanofiber creation methods is a formidable task without sacrificing certain characteristics. For example, in electrospinning the feed rate for the solution is set to a slow setting. This setting is chosen after multiple tests are done to determine which speed will produce fibers at a certain level of quality. If the feed rate is heightened, more fibers would be created, but the resultant fibers would experience inconsistencies in qualities sought for this process such as less fiber alignment, shorter fiber length, and improper evaporation of the solvent which leads to beading on the fibers and inconsistent fiber diameters. In recent years, a nanofiber production method has been created which grants an alternative way to increase fiber yield while maintaining the desirable qualities which come with each fiber production method. This method is known as electro-centrifugal spinning (EC-Spinning). There are different approaches to combining the electrospinning and centrifugal spinning methods, but the goals of the processes align very consistently. The desired

output is nanofibers which are aligned, have consistent and small diameters, and produce a much higher yield than typical electrospinning processes. This research will attempt to produce a hybrid process for creating nanofibers at high yields while keeping the high-quality properties which were previously mentioned. This method, also named hybrid spinning, will introduce the voltage potentials seen in electrospinning to a spinneret style centrifugal spinning setup and the resultant fibers will be compared through variation of parameters.

CHAPTER II

LITERARY REVIEW

Nanofiber creation methods have continuously improved over decades of research. Most fiber creation techniques are tailored to produce fibers with specific properties. Some of the phenomena seen in fiber spinning techniques date back centuries such as the Taylor cone detailed by A. L. Yarin et al. (Yarin, 2001). Other methods of fiber production are more recent such as Forcespinning™ which utilizes centrifugal forces to produce the elongated fibers rather than rely on electrostatic forces created by high voltage potentials (Trevino, 2021). The resultant fibers for each method vary significantly in terms of their properties. The hybrid process, which will be referred to as electro-centrifugal spinning, is meant to combine the two processes to achieve the creation of fibers that display the benefits each individual process has to offer. Different versions of this hybrid process have been created in recent years, each with a concentration on a different part of the fiber creation process.

Electro-centrifugal spinning, although fairly new, has been tested under varying conditions and parameters. In a study performed by Hosseinian et al. (2019) tested varying parameters using an 8 wt% solution of polyvinylpyrrolidone (PVP). The purpose of the experiments was to identify what changes the specimen would experience when the solution was spun under various conditions. The experimental setup consisted of a rotating cylinder which housed syringes containing the polymer solution. Using the centrifugal forces generated by the rotating motion, the solution was pushed through the nozzle of the syringe. An electrical field

was applied between the syringe and a collector to help stretch out and align the fibers once they were ejected. Characterization of the resulting fibers was done using an optical microscope, a scanning electron microscope (SEM), and X-ray diffraction (XRD). An operating diagram was developed which depicted the minimum operating conditions for the PVP solution to create nanofibers. If the parameters were below the curve, it would result in the creation of microparticles. Raising the voltage at constant rotational velocity had no effect on the ejection speed of the solution, but varying the rotational speed at constant voltage resulted in faster ejection from the syringe. A threshold was discovered where increasing the rotational speed would decrease the fiber diameter only up to a certain point. After reaching the threshold, the diameters began to increase. If the rotational speeds were too slow, the travel time of the fibers deceased which led to less time for the polymer jet to completely dry before reaching the collector. Optimal voltages for nanofiber creation were found to be between 6 and 10 kV and rotational speeds of between 2023 and 2428 rpm (Hosseinian, 2019).

In 2011, F. Dabirian et al. created experiments which tested the flow of solutions for each process. Dabirian described the setup to be a single container located within a disc with 2 mm of the nozzle protruding. Keeping the needle short will help control the forces experienced by the solution as the spinneret rotates. The team first calculated the flow rate in order to develop consistent testing parameters using centrifugal spinning at predetermined solution volume. They then applied that optimal flow rate to each test. The team tested the flow from centrifugal spinning of water which created a jet that would then break up into droplets. Applying electrospinning methods to the water resulted in the water spraying out rather than jetting. Using the combined electro centrifugal spinning process, the jet of water is formed from the syringe because of the centrifugal forces and the electrostatic forces elongate the stream before it again

turns into droplets. This reinforces the idea that electro centrifugal spinning does help create longer fibers under the same conditions given that it is able to have such effect on materials with low viscosity such as water. When compared with the water solutions, the polyacrylonitrile (PAN) tests performed under the same conditions resulted in the fibers being created with an increase in the alignment and a decrease in the diameter of the fibers when electro centrifugal spinning was used. Dabirian and team then tested a 16 wt% solution to check the results for fiber alignment, and compared to the previous tests which used 15 wt% PAN. The fibers presented a more uniform alignment. The images the team obtained of the solution leaving the needle displayed a jet shooting out in a straighter form since they were less susceptible to the bending instabilities which were found in the 15 wt% sample tests (Dabirian, 2011).

In a separate study performed in 2011, Dabirian et al. researched how varying the operational parameters of the electro-centrifugal spinning process affected the resultant fibers. The team ran experiments in which certain parameters were kept stagnant while they varied others and recorded the effects on the resulting fibers. The solution used was made up of polyacrylonitrile (PAN) powder dissolved in dimethyl formamide (DMF) solvent which resulted in concentrations between 13 – 16 wt%. A field-emissions scanning electron microscope (SEM) was used to characterize the fibers using an average of 100 different fibers. Flow rate for the solution was calculated by measuring the change in mass and dividing by the operating time of the electro-centrifugal spinning machine. The experimental setup consisted of a rotating disk capable of spinning at speeds of up to 10,000 rpm. The spinning disk contained two vessels which were used to hold the polymeric solution with a connected nozzle that protrudes slightly past the outer surface of the spinning disk. The purpose was to reduce the effects the air stream would have on the nozzle tip during rotation so the solution will not dry at the needle tip

preventing it from flowing freely. The voltages applied during the experiment were in the range of 0 to 22 kV and the collector was placed at a distance of 8 cm from the needle tip. The team used 0.3 ml of solution per run. The initial runs tested the effect of the voltage on the fiber diameter. The team saw no significant changes to the fibers leading to the conclusion that voltage has no effect on the diameter for their experiments. This varies from other research that has been performed, but it is important as it determined their testing setup for the next parts of the experiments. For the rest of the tests, a constant voltage of 15 kV was used. Through subsequent tests, it was determined that increasing the rotational speed while maintaining flow rate had a greater effect on the fiber diameter because it allowed the solution to dry faster before it stretched. The flow rate was adjusted by adjusting the nozzle length of the needle. When testing a changing flow rate at a constant rotational velocity, the results showed that when increasing the flow rate, the fiber diameter decreases. Allowing the flow rate to increase while increasing the rotational velocity initially reduced fiber diameter and standard deviation, but after a certain threshold, the diameter and standard deviation began to increase. Testing the effects of needle length on the fiber diameter, the team determined that reducing the needle length caused a reduction in fiber diameter. One final test compared the change in the concentration of the solution. The team tested concentrations from 10 to 16 wt% and concluded that increasing the concentrations increased the fiber diameter. The majority of the tests were run at speeds above 6000 rpm. (Dabirian, 2013)

Varied versions of the same electro-centrifugal setup have also been researched by other teams. Shu-Liang Liu et al. propose a modified version of novel Centrifugal Electrospinning process which would allow creation of nanofibers using smaller parameters in rotational velocity and voltage potential. The setup would include a rotating disk that would hold two syringes

facing opposite directions and needles that bent 90°, so the openings are facing down. The positive voltage is applied to the syringe needles, while the negative voltage is applied to an annular collector located directly below the needles. Materials used include polystyrene (PS), polymethyl methacrylate (PMMA), tetrahydrofuran (THF), and polyvinylpyrrolidone (PVP). Characterization of resultant fibers was done using scanning electron microscope and a fluorescent microscope. The purpose of the experiments was to improve fiber alignment using smaller operating parameters. In order to find optimal operating parameters, the paper states that the team set a common applied voltage of 6.2kV, a needle to axis distance of 16 cm, and a collecting distance of 3 cm. This allowed them to test varying rotational velocities and found an optimal range of 360 to 540 rpm, with 420 rpm being the most suitable for that voltage. When testing varying voltages at 420 rpm, the range required was found to be between 2.8 – 6 kV, and the collecting distance was optimized within 2 to 4 cm. The team also tested varying solution concentrations which affected the structure and morphology of the fibers. In conclusion, the paper stated that the team was able to get highly aligned fibers with optimal conditions at working voltage of 3kV, rotational speed 420 rpm, collecting distance 2.5cm, and solution concentration of 18wt%. Although they did produce highly aligned fibers, the low rotational velocity caused and increase in the fiber diameter to the micrometer range (Liu, 2013).

Taking note from previous research, the proposed electro-centrifugal spinning design will attempt to create a process for adjusting operating parameters while optimizing fiber properties and alignment. The hybrid spinning process should produce aligned nanofibers with small diameters and low standard deviation at to-be-determined optimal operating parameters.

CHAPTER III

DESIGN OF ELECTRO-CENTRIFUGAL SPINNING SYSTEM

In order to integrate electrospinning and centrifugal spinning to create the single electro-centrifugal spinning machine an existing setup was utilized and modified. The existing version of the hybrid spinning machine consisted of a first prototype of what was sought out in this research. Various components were changed out or removed in order to reduce design complexity of the system in exchange for reduced vibrations and more stable system performance. In the overall design of the machine, special considerations were taken in vibration reduction and in controlling the electrical fields which may cause interference while the fibers were being created. Specialized components were created utilizing 3D printing technology. This allowed the interface between components to be significantly simplified and created a more modular and adaptable process that can be repaired, maintained, and improved over time.

3.1 Electro-Centrifugal Spinning Machine Structure

When the goal is to create fibers in a hybrid spinning machine, a lot of hazards need to be considered and mitigated prior to starting production. One of the first major components needed to contain the setup is the enclosure. The structure is to have large enough dimensions to allow for collectors with varying diameters to be utilized. The frame of the enclosure is built out of aluminum extrusions bolted together with spaces for sectionalizing the various components, as shown in Figure 4. The overall dimensions of the enclosure are 2 ft in length, 2 ft in width, and 2 ft tall. The bottom-most layer of the machine houses the high voltage components which will be

detailed in a later section. The height of the lower compartment is 5- 9/16”. Separating the lower and middle compartments is a polycarbonate sheet slotted through the aluminum extrusions. The center compartment is the largest of the three. This is where the fibers will be produced and collected. The floor of this section will only be utilized to hold a 3D printed part that will not add any forces which can bend or damage the sheet. The large size initially was created to house large components such as a large collector, long coupler rods connected to the spinneret and attached bearings to help keep the coupler vertical. After redesigning it, the collector was relocated and the bearings were removed. The large space in this section remained as in the original system to avoid increasing the velocity of the air surrounding the spinneret that could affect the resulting fibers. Since the spinneret would be rotating at several thousand rotations per minute, is air movement within the enclosure so a larger volume would reduce the air flow that gets continuously propelled.

Figure 2: CAD assembly of enclosure shell structure.

Above the nanofiber collection chamber is a smaller compartment where the main components of the motor setup are located. These items are the heaviest parts of the setup and required a stronger material to keep the platform they are mounted on from bowing. A large sheet of ¾" plywood was used to make this platform as it would be easier to bolt components on it. Foam pads were used on the contact points in order to reduce the vibrations that can be transferred from the motor to the frame. The walls of the entire enclosure, including the door, are all made from polycarbonate sheets. The sheets themselves were chosen because of the properties that would help ensure the prototype could get through the testing phases without significant damage, and they have high electrical resistivity which was crucial to create a machine that is safe to use, and because they are transparent and allows the user to see what is going on in the process. Adapted to the different parts of the enclosure are various parts which were used for safety, functionality and wiring purposes. A detailed explanation of these items is presented in their respective sections in this chapter.

3.2 Motor Assembly

For the purpose which the machine is intended to be used, the motor being used for this setup is rated for 10,000 rpm. The motor assembly of the hybrid spinning machine which is located in the top compartment was reconfigured in the redesign. Initially the motor was mounted on an elevated platform, coupled with a rod that ran down into the spinneret aligned by two bearings and custom-made brackets. The motor was controlled by an Arduino which displayed the angular velocity and high voltages on a LCD screen on the front face of the enclosure. The system had multiple problems which were found in the initial testing phases. After replacing numerous devices such as IR sensors and the LCD, the decision was made to ask the user to measure the parameters by removing the microcontroller and utilizing a tachometer

and a voltmeter to determine the rpm and the high voltages being used. A voltmeter is used to measure the voltages from potentiometers that in a proportional way set the high voltages that create the electrostatic field, and also to measure the voltage from another potentiometer that sets the velocity of the motor and that through a calibration curve allows for the estimation of the rotational velocity of the motor and spinneret, see Figure 5. These changes allowed a lot of the complex wiring initially necessary to be eliminated and to simplify the system to concentrate on the other aspects of the EC-spinning machine.

Table 1: Motor input voltage (V) vs rotational velocity (rpm)

	Velocity (rpm)				
Voltage (V)	Run 1	Run 2	Run 3	Run 4	Run 5
0.25	330	374	383	384	387
0.5	710	754	755	764	735
0.75	1015	1060	1064	1074	1070
1	1308	1357	1362	1375	1375
1.25	1595	1651	1673	1681	1670
1.5	1882	1943	1960	1968	1960
1.75	2163	2225	2250	2261	2240
2	2486	2502	2533	2539	2523
2.25	2757	2780	2809	2806	2792
2.5	3024	3045	3083	3083	3063
2.75	3286	3310	3347	3347	3328
3	3545	3559	3608	3615	3589
3.25	3805	3811	3864	3869	3840
3.5	4054	4074	4101	4119	4087
3.75	4297	4309	4351	4365	4331
4	4544	4549	4592	4607	4574
4.25	4774	4789	4830	4834	4801
4.5	4997	5001	5045	5051	5022
4.75	5195	5209	5240	5242	5223
5	5341	5345	5374	5375	5349

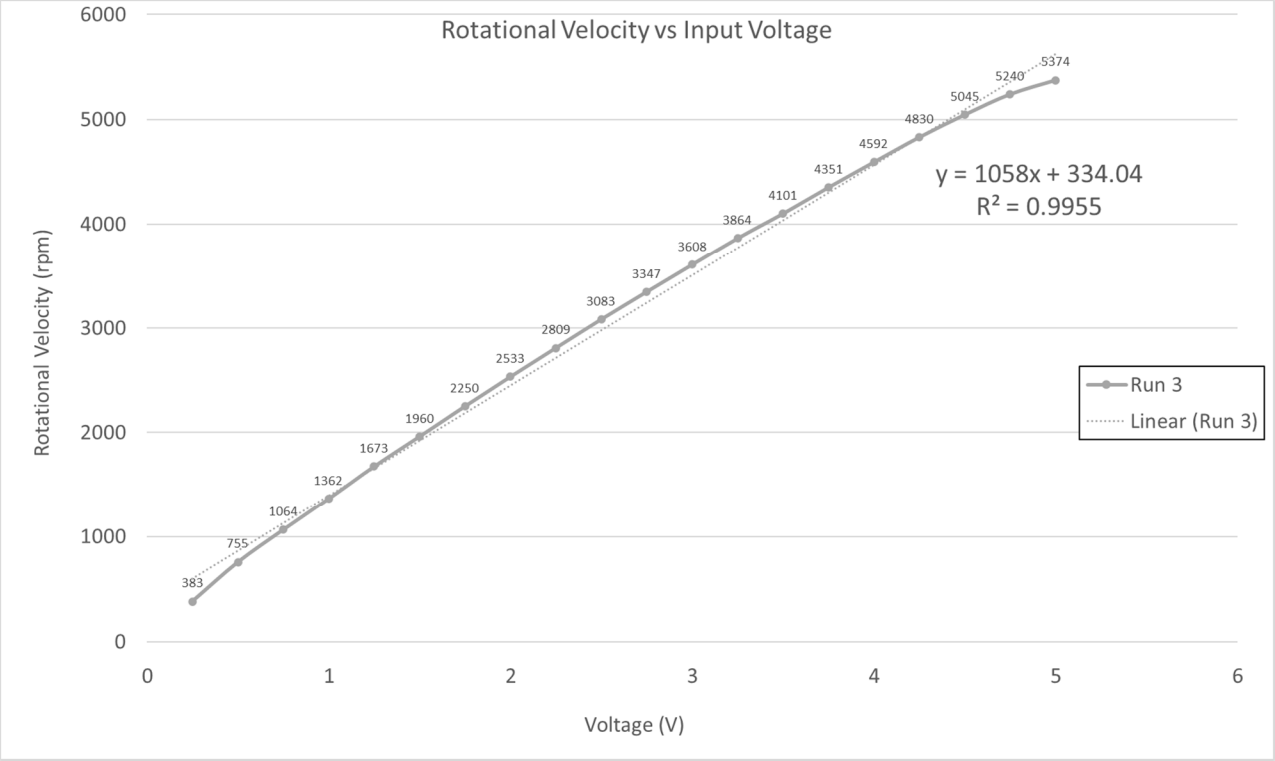

Figure 3: Chart relating motor voltage input to rotational velocity. Linear trendline shows a coefficient of determination (R2) value of 0.9955.

Calibrating the rotational velocity of the motor as a function of the input voltage out of a potentiometer required multiple runs to allow the motor to heat up and diminished the differences in velocity during each run. The voltage from the potentiometer is applied to the brushless DC motor driver that powers the motor using a 48Vdc power source. The data gathered showed a linear relation between the input voltage and the rotational velocity of the motor, particularly between 0.75V to 4V. The desired testing parameters for the EC-spinning setup with respect to rotational velocity are between 1000 rpm to 4000 rpm. This allows the creation of a linear trendline

$$\omega = 1058(V) + 334.04 \qquad (E.1)$$

where □ is the rotational velocity in rpm and V is the input voltage from the potentiometer. With this equation (E.1), the operating velocity of the motor can be prepared prior to starting the machine.

A major issue which could create problems for any fibers produced by the machine was due to vibrations. The complex interface between the motor and the spinneret could create vibrations because of unbalanced conditions or misalignment and such vibrations are transferred to the needles where the solution come out. To mitigate such issues, the setup was significantly modified and simplified. The motor was mounted directly to the base board of the top compartment with the threaded shaft of the motor falling directly into the middle compartment where the fibers are created. In order to connect the spinneret to the motor, the spinneret was redesigned to include a direct connection to the motor shaft utilizing the threading. The specifics for the spinneret will be discussed in a later section. The new simplified setup eliminates any problems that come from utilizing couplers, bearings, and other attachments.

3.3 High Voltage Power Supplies

The electrospinning components of the EC-spinning machine setup primarily include the high-voltage power supplies, the collector with high conductivity, and proper connectivity between all parts. Properly separating the power supplies and routing the wires to the collector and the spinneret was of high importance to avoid unwanted electrostatic fields that might misdirect the produced fibers from the intended collector. The high voltage power supplies used for this setup could each generate potentials of up to 10,000 Vdc for their respective polarity netting a maximum voltage potential difference of 20,000 Vdc. The positive power supply is located at the center of the base below the spinneret. This allows to make the connection to the spinneret with the minimum possible distance. The cable which is route to the bottom of the

spinneret, goes through a 3D printed tower which houses a carbon brush loaded with a spring right under the spinneret to maintain the contact while the spinneret is rotating. The spring provides a force that pushes the carbon brush into the bottom cup of the spinneret which has a copper piece that at the same time extend to make contact with the needles. Therefore, the positive high voltage is applied to the needles. The negative power supply is placed on the far-left corner of the compartment and a cable is routed straight up into the fiber collection compartment which then cuts towards the center of the chamber attaching to a wire ring located on the circumference of the collector using an alligator clip. Keeping the wires providing the high voltages to the spinneret and the collector apart is important as it reduces the possibility of creating undesired electrostatic fields and misdirecting the fibers traveling from the spinneret to the collector.

The initial setup for the hybrid spinning machine had a separate Arduino microcontroller gathering data from the power supplies and displaying it using an LCD screen on the front of the enclosure. After extensive troubleshooting steps, it was decided to remove the automated measuring devices and instead use resistors in series as voltage dividers to reach measurable volage levels which can be read using a multimeter. Given that the maximum voltage potential of each power supply is 10,000V, a 1 MΩ resistor and a 100Ω resistor were placed in series for each power supply and each was connected to their respective measuring posts on the face of the enclosure. Utilizing the formula for a voltage divider, resultant high voltage can be determined by measuring a much lower voltage,

$$V_{R_2} = \frac{V_{in}(R_2)}{R_1 + R_2} \qquad (E.2)$$

Plugging in the maximum value of the high voltage,

$$V_{R_2} = \frac{10{,}000V(100\Omega)}{1{,}000{,}000\Omega + 100\Omega} = 1V \qquad (E.3)$$

Therefore, any voltage between 0 and 1V measured at the measuring post is proportional to the 0 to 10KV voltage out of the high voltage power supply. In a similar way the negative high voltage is measured.

In summary, the high voltage power supplies require potentiometers to adjust the output voltage used to create the electrostatic field in the system. Voltage dividers are used to reduce output voltage to levels low enough to measure through common tools such as multimeters. As an example, a 0.5V measurement on the voltmeter would signify the total output on the power supply is 5,000V. Once the values for each output were verified and tested multiple times with consistency, the wires were routed properly.

3.4 Spinneret Design

Figure 6 shows the final spinneret design.

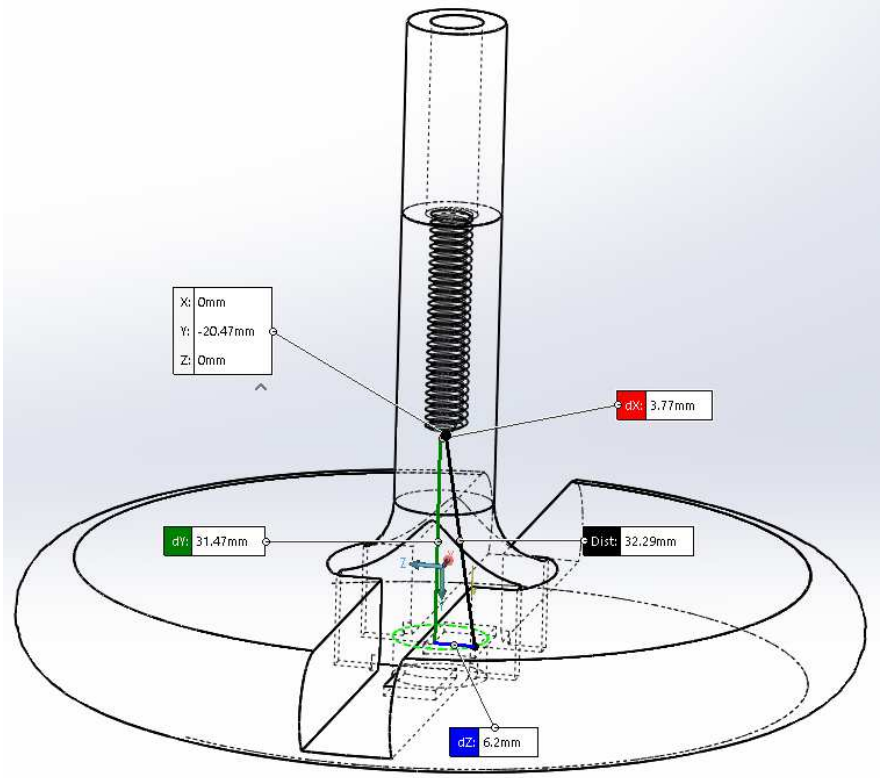

Figure 4: CAD model of spinneret showing the thread required to connect it to the motor, a 31.47mm distance between the end of the shaft of the motor to where the positive high voltage would be; and with compartment to insert the syringe holders.

Designing a new spinneret version was one of the main goals of this project and it was required to improve the performance in comparison to the previous spinneret. The main goals for the new version had to include material that was non-conductive, it had to carry more solution than a typical electrospinning setup, and it had to adapt in a simple manner to the motor shaft and the carbon brush that provides the high voltage. It also required compartments to insert and remove the syringe holders in a practical way. A natural solution that was agreed upon was to use 3D printed materials with custom designed models. Many concepts were created and adjusted at every iteration, taking the best results of each version. Having the freedom of designing a proprietary model allowed the opportunity to include a threaded hollow shaft which could screw onto the motor shaft, with buffer material to create a separation between the end of

the shaft and the positive high voltage input coming from under the spinneret as can be seen in Figure 5. This space was required to keep distance between the high voltage and any motor part.

The previous version of the spinneret that was used in the hybrid spinning machine had a compartment which would hold a small drop of solution in each side that was to be processed. This limited the number of fibers that could be produced and made cleaning afterwards a difficult task. For the current design, a cartridge approach was taken using syringes that are cut to size so they could fit into new cartridge compartments. The cartridge dimensions were made to fit tightly into a slot on the spinneret and lock in place by pushing outward. Adjusting the design to the new version of the system allows users to change out syringes that were already prepared, make cleaning after each session easier, and reduce the down time significantly.

To ensure continuity of the circuit from the positive high voltage to the tip of the syringe needle channels were included in the spinneret design which allowed a combination of thin copper strips, double-sided copper tape and micro-fiber steel wool to charge up the solution being processed. In the bottom part of the spinneret right at the center is an opening leading into the base 14.5 mm in diameter and 6 mm deep. Both sides of the cutout contain openings perpendicular to the cartridge channels 3 mm from the bottom surface of the spinneret. This opening allows a strip of copper to be run across the center of the spinneret connecting both cartridge channels together. The carbon brush will be pressed against the center of this strip to connect the spinneret to the high voltage. Between the copper strip and the spinneret, a foam thermal pad was placed to insulate the spinneret plastic from any heat generated as the static carbon brush and the dynamic copper strip interface during fiber creation. To keep the brush from touching the side walls of the hole on the spinneret and to increate contact points between the brush and the copper inside the spinneret a 14.5 mm outer diameter copper tube with 12 mm

height was used. Using the copper tube instead of a 3D printed coupler increased the durability and electrical conductivity of the spinneret.

Up to this point, once in place the spinneret is mounted to the motor with a positive high voltage continuously conducting through the spinneret and out into the cartridge channels using the copper strip. To get the voltage from the copper strip to the tip of the syringe needle an interface was necessary. Within the cartridges, where the syringe would go, a strip of double-sided copper tape was placed from the front opening of the cartridge where the needles would protrude, through the inside surface running along the bottom staying as close as possible to the contour of the cartridge. This was to avoid any tears on the tape when inserting and removing the syringes. Towards the back of the cartridge, an opening allows the tape to be continuously fed to the outside bottom face to serve as a contact point between the copper strip on the spinneret and the cartridge once it is seated in place. Continuity is then tested using a voltmeter by setting the cartridges in place and touching the copper tube under the spinneret, and the tape strip located inside the cartridges individually.

The final contact point to finalize a continuous circuit from the high voltage power supply to the tip of the syringe needle were the boundaries between the syringe and the tape strip running through the inside of the cartridge. Initially, to solve this problem the syringes and needles were selected entirely of metal. Although this would serve the purpose, it was expensive since the needles were sometimes damaged when being fed through the cartridge, were difficult to clean after each run, and were expensive and difficult to get. The alternative solution which was used included utilizing plastic syringes and fine steel wool to create contact points with the needles. The typical needles that are used for syringes have a plastic base, but the needle itself is metallic. By placing steel wool inside the cartridge compartment towards the front where the

needle goes through, contact points between the wool and the needle are created. At the same time the wool makes contact with the tape strip inside the cartridge thereby completing the intended circuit up to the needle where the solution would pass through. Once again, a voltmeter was used to verify circuit continuity from the power supply up to the needle of each syringe.

3.5 Modular Collector

On the opposite end of the intended electrostatic field will be a collector which is charged with a negative high voltage powers supply. The collector that is used in this setup was designed to be modular to expand the parameters that can be adjusted when testing the new hybrid system. Most notable is the diameter adjustment capability built into the 16 spoke design. Using CAD and 3D printing, a circular grid was created with slots located at every 25.4 mm. A circular track allows the pins to be inserted using the rectangular head and rotated to lock into place. Intermediate spokes were added between the initial 8 that allowed additional slots to be staggered 12.7 mm which doubled the possible adjustment options for the radius of the collector. The new collector design is screwed to the top part of the fiber collection chamber ensuring the slots for the pins were facing down. Because of printing size constraints, the collector grid was printed in quarter panels and assembled in the center of the chamber around the motor shaft.

Bottom face of collector base quarter pannel displaying pin head travel channels.	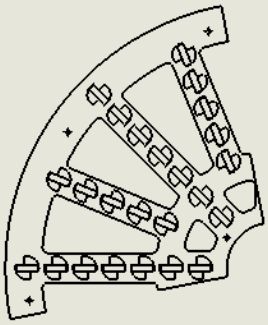
Top face of collector base quarter pannel displaying pin head insert slots.	
Isometric view of collector base bottom face quarter pannel displaying pin head travel channel depth.	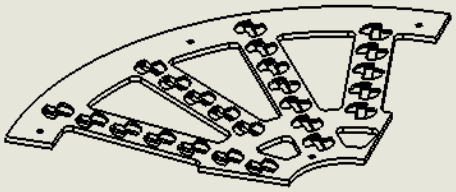

Figure 5: Drawing views of collector quarter panels showing slots for pin head and running track for pin rotation.

The pins that attach to the notches on the grid are modeled and 3D printed to fit tightly once in place to limit movement. One face of the pin is flat where a collecting sheet would be placed facing the motor shaft. The other side of the pin contains a hook that is designed to hold a copper wire that loops around the circumference of the pins. The alligator clip that is attached to the negative high voltage power source is connected to this copper wire. The top part of the pin has a rectangular slab the same width as the pin, 1.8 mm thick and 16 mm in length attached with a cylinder between the base of the pin and the head. This allows the pin to rotate with no

interference. Using the various slot distances on the grid, the pins can be placed to test fiber creation at multiple distances between the needles and the collector.

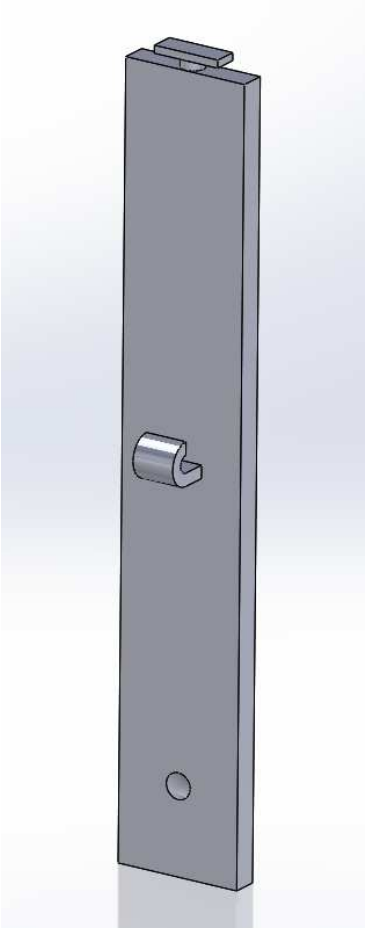

Figure 6: Collector pins CAD model with hook for collector negative high voltage wire.

3.6 Safety Features

User safety is crucial for operation of the EC-spinning machine as there are elements that can be dangerous to be around if no precautions are set in place. Injuries stemming from the high voltage power sources, mechanical damage to spinning parts that could launch items at high velocities, or even chronic damage caused from working around nanofibers are all real possibilities and have been taken into account for safe use of the machine. One of the immediate

hazards of the setup is working around high voltages. Special considerations were taken in the placement of the power supplies in reference to the user and other conducting surfaces, but additional hazard mitigation steps were taken to keep the user safe. One automatic fail-safe was integrated into the motor circuit. This being a pair normally closed switches which prevent the motor from operating and turns off the high voltage power supplies if the door to the enclosure is open. The switches, also known as Reed switches, use a magnetic actuator that will close a circuit when the two switches are close to each other. For each individual circuit, a 5V power supply cable is routed from a 12V power source onto a toggle switch that will turn the power to each component on or off. To ensure the circuit is open when the door opens, the 5V cable is routed from the output of the switch, up to the normally closed switch and then back again towards the high voltage power supply. This will ensure the power is cut to all elements when the doors open. An additional emergency button is utilized which can also help stop the motor and high voltage power sources in case of a fire or other immediate emergency that may happen.

Figure 7: Normally closed switch that will disable motor circuit when separated.

Figure 8: Emergency stop button that cuts power to the motor and high voltage power supplies.

Hazards created by the rotational velocity of the motor were also considered. As mentioned in the enclosure section, the fiber collection chamber needed to have strong enough walls to withstand impact from any part that may have dislodged during rotation. The design of the spinneret and cartridge include elements such as locking mechanisms to keep the cartridge and syringe in place while they are spinning. As added precaution, the material used for the walls still needed to be strong enough to withstand the impact of the plastic cartridge launched by a motor spinning at 10,000 rpm. The polycarbonate sheets used are rated for impact strength between 12 - 16 ft-lb/in. With conservative calculations, the maximum impact force that can be created by the cartridge launched at the maximum 10,000 rpm for which the motor is rated. Converting 10,000 rpm to rad/s results in a rotational velocity of 1047.2 rad/s. Calculating the tangential velocity for the spinneret traveling at this speed can be done so using

$$V_t = r * \omega \qquad (E.4)$$

where V_t is the tangential velocity, r is the radius of the spinneret, and □ is the rotational velocity. A maximum radius of 76.2 mm or 0.0762 m can be used as it provides an additional factor of safety. Plugging in the values results in a maximum tangential velocity of 79.8 m/s.

$$V_t = 0.0762m * 1047.2\frac{rad}{s} \qquad (E.5)$$

Using the kinetic energy formula

$$K_E = \frac{1}{2}mv^2 \qquad (E.6)$$

the maximum possible energy which can be attained can be calculated where K_E is the kinetic energy, *m* is the mass of the loaded cartridge with the syringe and solution included, and *v* is the tangential velocity which was already calculated. Using 10g or 0.01kg for the mass, which is much higher than the total weight of a fully loaded cartridge the following calculations can be performed

$$K_E = \frac{1}{2}0.01kg * (79.8m/s)^2 \qquad (E.7)$$

which results in 0.399 Joules (J). Using a conversion table which relates 1 J to 8.850746 lbf-in, the resulting kinetic energy is 3.531 lbf-in or 0.294 ft-lb. Dividing the calculated kinetic energy by the maximum distance traveled of 12 inches will result in the maximum possible impact force of 0.0245 ft-lb/in if there are no deformations. To conclude, the maximum possible exerted force of a dislodged spinneret loaded with a syringe, needle, and solution is within the limits of what the polycarbonate sheets can handle.

In the fiber spinning phase of the process, the fibers are created when the solvent used in the solution evaporates leaving only the polymer to be stretched by both the centrifugal and electrostatic forces. The evaporated solvent does impose a hazard which can vary in severity depending on the solvent utilized. In the initial testing phases of the setup, PEO was used as the solvent used to create the solution is water. This helps minimize the hazard of potential fumes

which can affect the users. In preparation for more hazardous solutions which will also be spun for their properties, a fume hood is used on the back panel of the fiber collection chamber which leads to a collective manifold located in the lab. This will also help absorb all leftover nanoparticles which may not have landed on the collector.

Figure 9: Fume hood used to exhaust evaporated solvent and nanoparticles which do not attach to collector.

CHAPTER IV

EXPERIMENTAL PROCESS AND TESTING

4.1 Solution Preparation

Material selection for testing the hybrid spinning machine was an integral part of ensuring proper functionality of all the systems involved. The first solution preparation consisted of a polymer that would be water-soluble, non-toxic, and have high ionic conductivity. Polyethylene Oxide (PEO) properties meet all of the criteria making it the best candidate to work with on the hybrid spinning machine. The solution used has a molecular weight of 900,000 g/mol. For these particular tests, the solution used contained 8% concentration of PEO mixed in with deionized (DI) H2O. Once measured, the solvent and the polymer are mixed into a homogeneous solution using a vortex mixer to agitate the dispersion. The solution is then placed in a bath Sonicator to allow any agglomerates and air bubbles to disintegrate. Once this process is completed, the solution is placed in a stirring plate overnight. Next, the solution is characterized prior to testing. A Rheometer was used which resulted in a viscosity (η) between 50,000 to 55,000 centiPoise (cP). While characterizing the viscosity, the solution had a stable period at a shear rate between 0.1 to 0.5 γ in 1/s, then the viscosity decreased to around 3,000 cP.

Following the viscosity characterization, the team then measures the density. Density characterization is an important factor which helps understand the composition of the solution. The calculated density for this particular solution was 1.0795 g/cm^3.

The final characterizing step for the solution is to measure the surface tension using the FAMAS (interFAce Measurement and Analysis System) machine. The surface tension helps observe the shape of a solution droplet and measure the drop volume as well as the droplet's height and width. Running the solution through this test resulted in the 8% PEO solution showing an average surface tension of 64.4 N/m.

4.2 Machine Initialization

Once the solution is ready to be processed, the hybrid spinning machine is prepared to run. An important step to help ensure consistent results is to warm up the motor. Using equation E.1 in Section 3.2 of this paper, the desired velocity can be calculated. Turn the potentiometer knob until the calculated voltage is reached. Running the motor for at least 10 minutes prior can help stabilize any fluctuations in rotational velocity.

While the motor is heating up, the solution cartridges can be prepared. The syringes which will be placed in the cartridges can hold 1 mL of solution. The cartridges with the syringe in place can be loaded onto the spinneret, all the while taking special precautions with the protruding needles. Ensure to lock in the cartridge by pulling away from the spinneret.

An important parameter that should be considered any time nanofibers are to be tested is the room humidity. It has been seen that at higher humidity levels, the nanofiber creation processes experience fluctuations in the quality of the fibers. Changes such as lower nanofiber production yield, less solvent evaporation, and fiber diameter and length are less consistent. For ideal conditions, it has been seen that a room humidity of around 50% will produce proper results. Therefore, it is important to take a measurement of the room humidity prior to beginning the testing process.

At this point, the user can adjust the distance between the needle and the collector to the desired value. The collector base has two tracks which allow adjusting this parameter by ½" increments. The cable providing the negative high voltage can be set in place and connected to the negative high voltage power supply using the alligator clip coming from the power source.

The final part of the hybrid spinning machine setup process is to set the high voltages. Turn on the toggle switch for the high voltage power supplies. Using a multimeter, take a reading across the respective voltage posts. This voltage can be adjusted using the potentiometer located on the same side as the toggle. The output voltage of the high-voltage power source is 10,000 to 1 to the voltmeter reading. For example, if the desired voltage is -5,000V, the multimeter should read -0.5V. Repeat the steps with the positive high-voltage power source. After the voltage has stabilized on the multimeter the setup is complete and the fiber creation process can begin.

4.3 Creating and Collecting Fibers

Once the electro-centrifugal spinning machine has created fibers, the fibers will need to be collected and labeled. Using glass slides, the operator will collect fiber samples. Place the slides with the collected fibers into a small zip lock sample bag and label it using permanent marker. The label should include the testing parameters. For the PEO samples, the team wrote the solution concentration, the humidity in the room, the time the machine ran for, the voltage settings for the high-voltage power supplies, the rotational velocity of the motor, and the date the test was run.

At this point, the collector pins will need to be changed or cleaned prior to beginning the next run. While the pins are out, the operator can now remove the cartridges from the spinneret by carefully pushing the cartridges towards the center of the rotational axis and lifting the cartridges up. This step needs to be done carefully to avoid any punctures from the needles. A

tool such as a flat head screwdriver can be used to help lift the cartridges. These steps can be repeated for as many runs as the testing process requires.

4.4 Fiber Characterization and Measurement

The characterization process for the created nanofibers begins with preparing the samples for Scanning Electron Microscope (SEM) imaging. This process scans the surface of the produced samples using a beam of electrons and provide information about the surface topography and composition. The samples should be cut to size and placed in specimen stubs which are used to load onto the SEM. When the samples are in place on the specimen stubs, they are taken to the sputtering machine which will coat the fibers with a conductive metal such as chromium, platinum, gold or silver. This is necessary to avoid having the SEM burn the fibers. Once sputtered, the samples can be taken to the SEM. The specimen stubs holding the fibers are then placed into an SEM pin mount and screwed in. Prior to placing the SEM pin mount in, the SEM needs to be vented using nitrogen to purge the whole machine. Without this step, the electrons that are aimed at the sample can hit an air particle which would then damage the SEM. Once the samples are in the SEM, nitrogen will need to be pumped into the SEM to purge the testing chamber.

Using the SEM software, the images can be taken and saved, making sure to properly label samples. When all the images have been collected, the SEM can be purged using Nitrogen and powered down.

The final step of characterizing the samples is to take measurements of the fibers in the images gathered using the SEM. To do this, a software called Image J is used. Within the software, the images from the SEM are opened and within the image, the scale provided by the SEM is used to set the standard for the measurements of fiber diameters or lengths that are taken.

For each image, a new scale will need to be set as the magnification might change from image to image. The measurements are then taken for various fibers within the image measuring the diameter of the fibers. After enough points are found, the data is tabulated and exported to an Excel file. From this point the data can be compared and analyzed.

CHAPTER V

ELECTRO-CENTRIFUGAL SYSTEM TESTING RESULTS

This chapter summarizes the initial results of the developed electro-centrifugal system. The following sections describe the yield obtained with different operating parameters and the characterization of the fibers produced by the system. The material system selected was polyethylene oxide (PEO) at 8 wt% concentration. The processing parameters were 0 – 4000V potential, 2000 – 4000 rpm rotational velocity, and a 6 cm distance between the needle and the collector. The collected fibers were characterized and analyzed in terms of yield, fiber diameter, and fiber orientation.

5.1 EC System Fiber Production Yielding

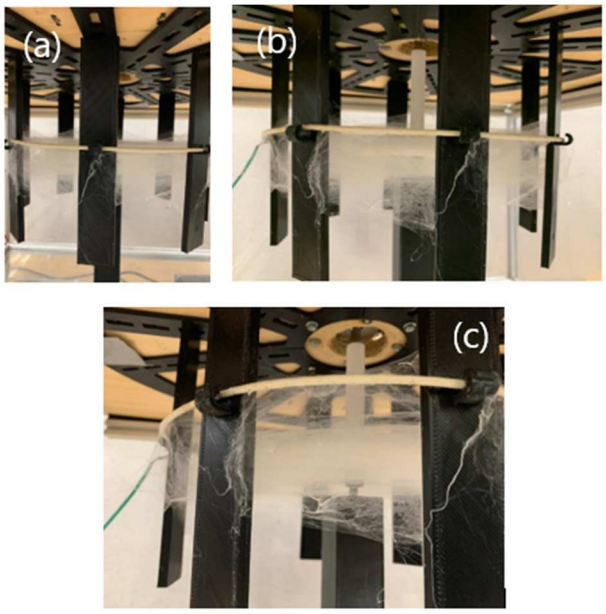

Figure 10: Fibers collected using 8 wt% PEO in DI H2O rotating at 4000 rpm and (a) 0V, (b) 2000V, (c) 4000V potential.

Table 2: Measured production yield for each combination of test parameters in g/hr.

	Voltage Potential		
Rotational Velocity (rpm)	0V	2000V	3000V
2000	0.048	0.06	0.06
3000	0.204	0.24	0.252
4000	5.58	6.096	6.612

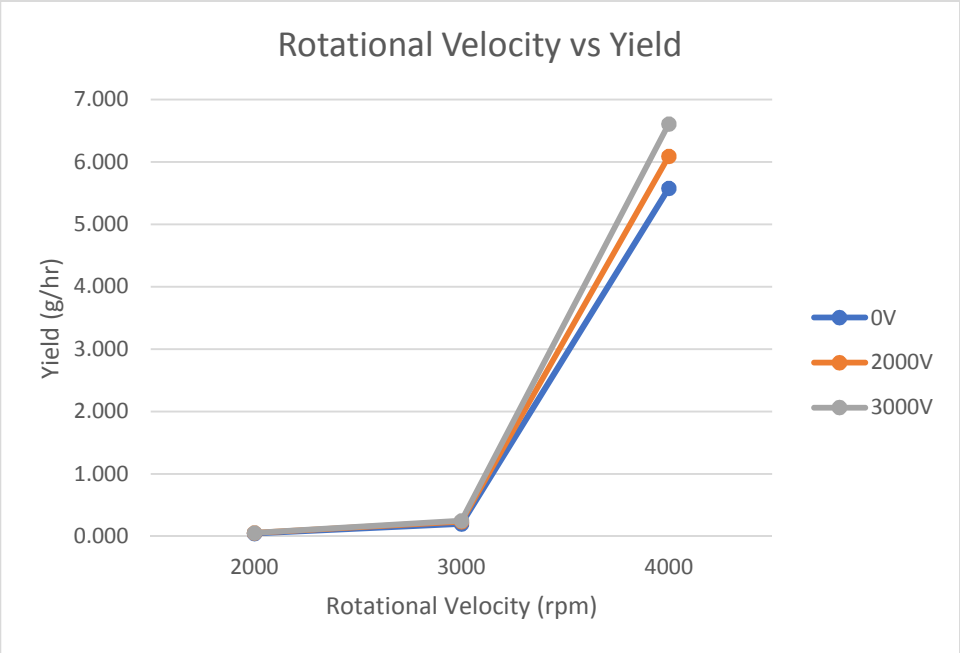

Figure 11: Visual representation of rotational velocity vs production yield at each voltage potential.

The yield for each run was heavily dependent on the rotational velocity. At lower velocities, the electro-centrifugal spinning machine produced low quantities of fibers and had to be run for longer periods of time in order to obtain a large enough sample to test. When adding the high voltage inputs, there was an increase in the measured yield (10-25%). At 2000 rpm, the difference between samples with and without high voltage inputs was only 0.012 g/hr where runs that included high voltage inputs produced more fibers (25% more than no electric field). At

3000 rpm the difference increased to 0.036 g/hr and 0.048 g/hr with the different electric fields (18% and 24% more than no electric field), again with the non-zero high voltage input runs producing more fibers. At the highest production rate, the 4000 rpm runs were producing fibers at over 5.5 g/hr. The difference between runs with a voltage input and those without were higher by 0.516 g/hr and 1.032 g/hr (9% and 18% more than no electric field).

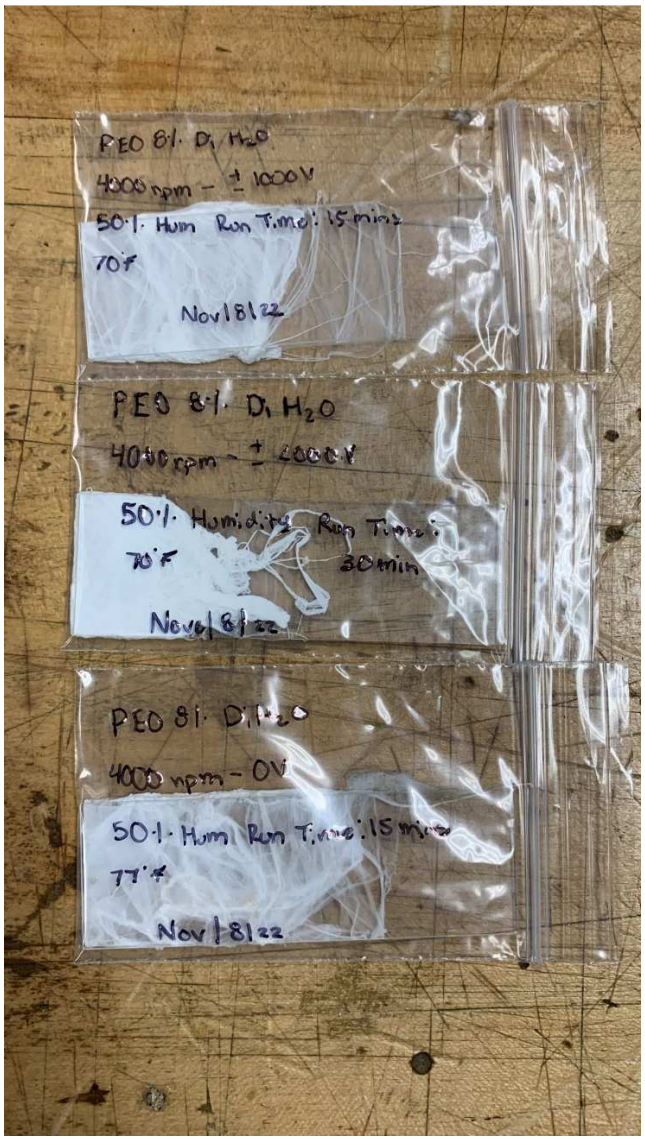

Figure 12: Collected PEO nanofibers at 4000 rpm with testing conditions labeled.

5.2 EC Fiber Characterization

The produced fibers were collected in glass slides and prepared to be viewed through a scanning electron microscope. The following images were produced.

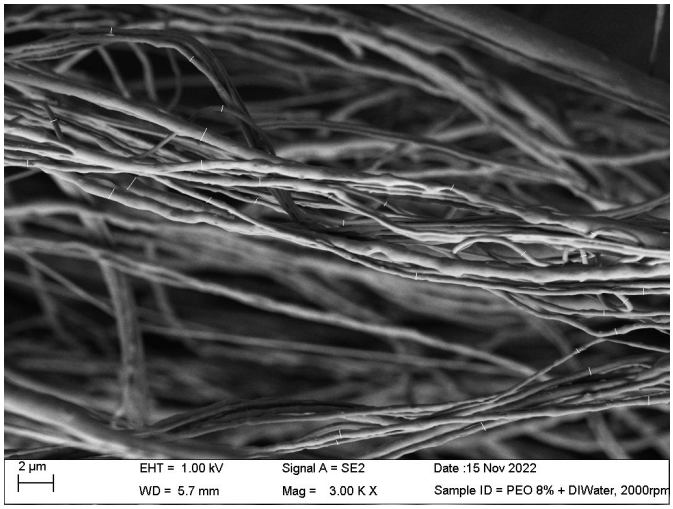

Figure 13: 3000X Magnification 8 wt% PEO in DI H2O at 2000 rpm and 0V

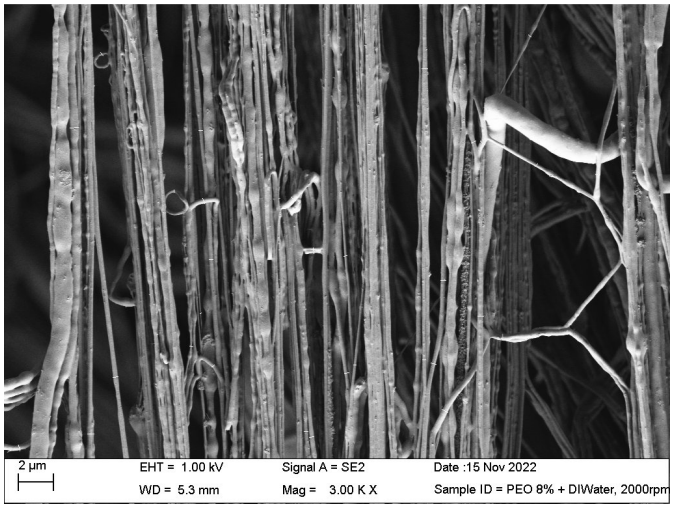

Figure 14: 3000X Magnification 8 wt% PEO in DI H2O at 2000 rpm and 2000V

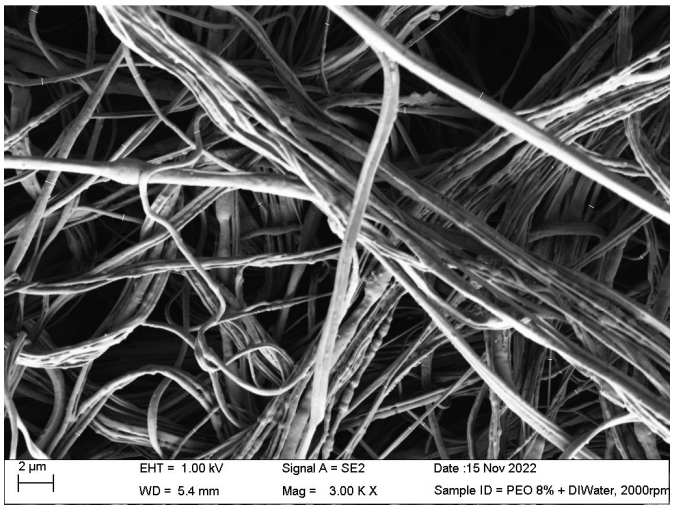

Figure 15: 3000X Magnification 8 wt% PEO in DI H2O at 2000 rpm and 4000V

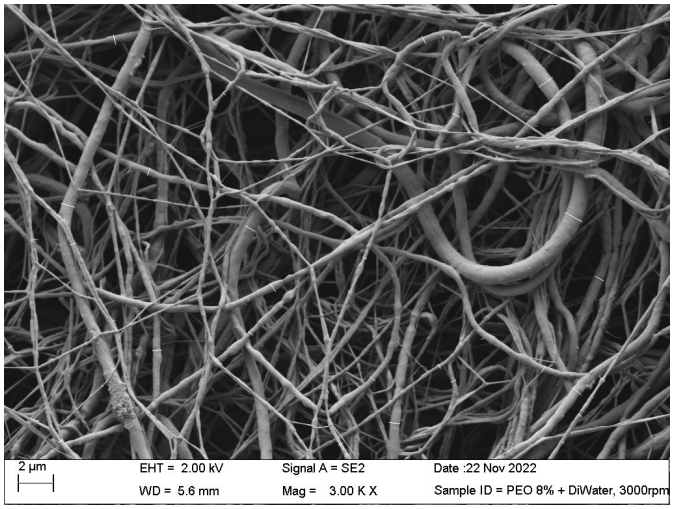

Figure 16: 3000X Magnification 8 wt% PEO in DI H2O at 3000 rpm and 0V

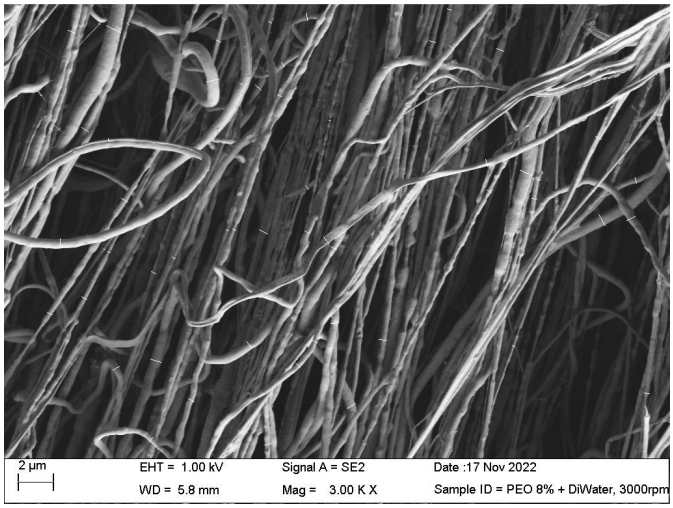

Figure 17: 3000X Magnification 8 wt% PEO in DI H2O at 3000 rpm and 2000V

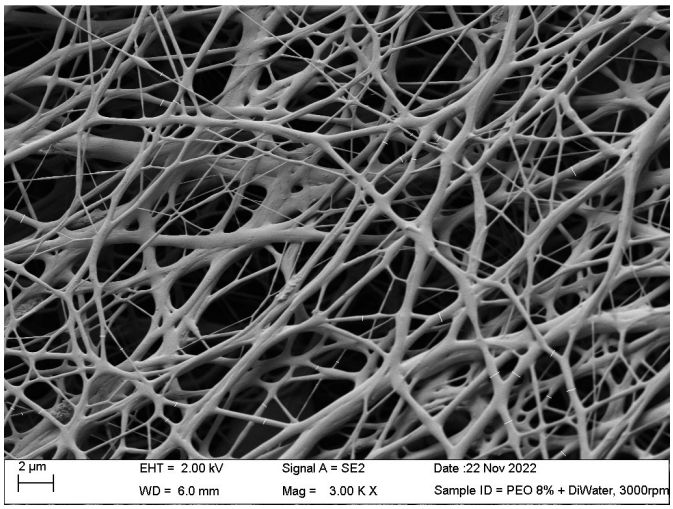

Figure 18: 3000X Magnification 8 wt% PEO in DI H2O at 3000 rpm and 4000V

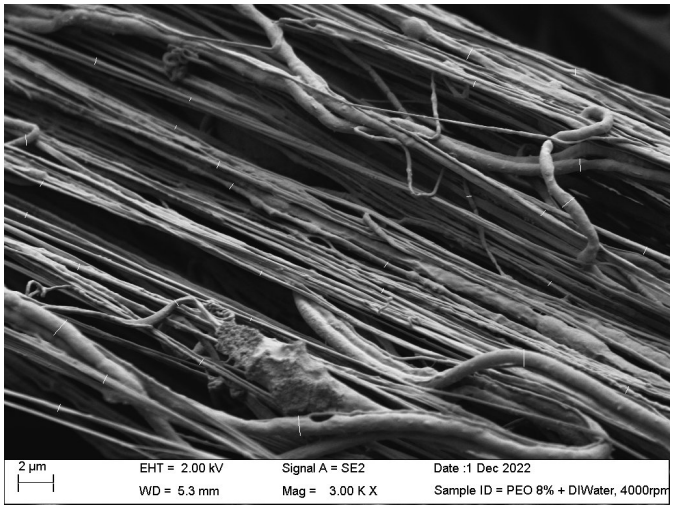

Figure 19: 3000X Magnification 8 wt% PEO in DI H2O at 4000 rpm and 0V

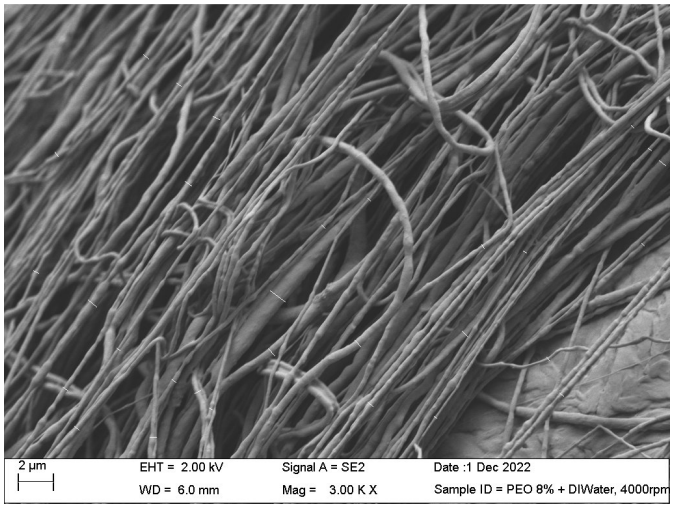

Figure 20: 3000X Magnification 8 wt% PEO in DI H2O at 4000 rpm and 2000V

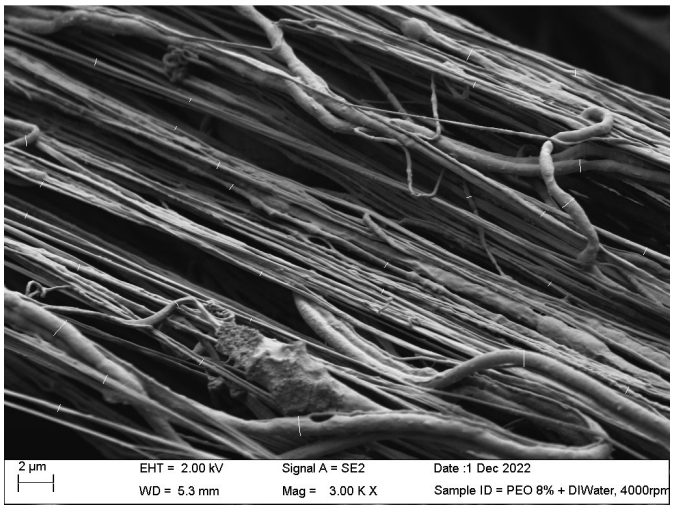

Figure 21: 3000X Magnification 8 wt% PEO in DI H2O at 4000 rpm and 4000V

A total of 30 fiber measurements were taken at random points for each image. The average and standard deviation was calculated for each voltage level for each rotational velocity. The produced fibers were in the low 100s of nanometers to the micrometers range. The normal distribution was mapped for each voltage level to display how voltage changes affected the resulting fibers. Trends were found for all rotational velocities which displayed a decrease in fiber diameter and standard deviation when a voltage was applied. At 3000 rpm and 4000 V potential there was an increase in the measured humidity. The change in operating conditions affected the fiber yield and fiber quality as can be seen in Figure 18 above. While fibers displayed the quality improvement trend that was expected when adding a voltage, the produced fibers were melded together creating a fiber interlocking effect (i.e., fusion of fibers at the intersections).

Mapping out the normal distribution using a bell curve shows the trend change the produced fibers experienced when a voltage was added. In all three rotational velocities, the 0 V runs had a wider bell curve than the curves representing runs with a higher input voltage. This is representative of the induced reaction between the PEO solution used and the positive high voltage input that was applied. The data shows that the smallest fiber diameters were produced at lower rotational velocities. Increasing the input voltage while maintaining a low rotational velocity can help reduce the fiber diameters but will produce low fiber yield quantities.

Table 3: Measured fiber diameters created at 0V, 2000V and 4000V potential for each of the rotational velocities (2000 rpm, 3000 rpm, 4000 rpm).

	2000 rpm			3000 rpm			4000 rpm		
	0V	2000V	4000V	0V	2000V	4000V	0V	2000V	4000V
	0.815	0.264	0.439	0.575	0.558	0.296	1.134	0.501	0.233
	0.55	0.303	0.597	0.286	0.344	0.171	0.184	0.426	0.226
	0.394	0.345	0.348	0.812	0.629	0.239	0.382	0.345	0.129
	0.319	0.348	0.387	0.338	0.367	0.299	0.199	0.42	0.196
	0.357	0.235	0.396	0.585	0.352	0.377	0.703	0.361	0.28
	0.415	0.191	0.366	0.252	0.786	0.304	0.394	0.338	0.335
	0.341	0.291	0.277	0.132	0.379	0.292	0.269	0.249	0.2
	0.351	0.373	0.323	0.301	0.435	0.139	0.427	0.256	0.254
	0.36	0.189	0.298	1.134	0.403	0.27	0.4	0.187	0.195
	0.302	0.207	0.238	0.412	0.305	0.574	0.38	0.312	0.36
	0.379	0.229	0.373	0.27	0.915	0.622	0.982	0.242	0.337
	0.367	0.334	0.216	0.28	0.463	0.386	0.362	0.202	0.256
	0.323	0.406	0.214	0.445	0.405	0.164	0.253	1.046	0.203
	0.224	0.354	0.162	0.541	0.344	0.311	0.284	0.558	0.319
	0.515	0.287	0.342	0.465	0.717	0.364	0.201	0.337	0.257
	0.696	0.188	0.24	0.146	0.369	0.273	0.459	0.289	0.511
	0.356	0.225	0.186	0.534	0.279	0.364	1.113	0.641	0.202
	0.368	0.26	0.214	0.684	0.537	0.397	0.274	0.282	0.257
	0.867	0.24	0.208	0.217	0.415	0.193	0.587	0.21	0.712
	0.362	0.343	0.189	0.302	0.451	0.382	0.406	0.523	0.122
	0.429	0.272	0.427	0.96	0.526	0.225	0.872	0.214	0.372
	0.316	0.114	0.322	0.321	0.452	0.122	0.295	0.371	0.332
	0.408	0.395	0.253	0.284	0.726	0.518	0.702	0.373	0.269
	0.235	0.322	0.163	0.51	0.248	0.417	0.315	0.322	0.303
	0.375	0.285	0.155	0.394	0.482	0.525	0.331	0.376	0.318
	0.267	0.347	0.374	0.244	0.31	0.642	0.556	0.422	0.441
	0.502	0.348	0.234	0.327	0.45	0.556	0.394	0.235	0.438
	0.301	0.511	0.201	0.657	0.296	0.518	0.31	0.235	0.508
	0.502	0.199	0.193	0.421	0.352	0.382	0.399	0.494	0.312
	0.336	0.258	0.351	0.446	0.564	0.294	0.412	0.27	0.418
Average	0.411067	0.288767	0.289533	0.4425	0.461967	0.353867	0.465967	0.3679	0.309833
Max	0.867	0.511	0.597	1.134	0.915	0.642	1.134	1.046	0.712
Min	0.224	0.114	0.155	0.132	0.248	0.122	0.184	0.187	0.122
Range	0.643	0.397	0.442	1.002	0.667	0.52	0.95	0.859	0.59
Std. Dev.	0.151633	0.082249	0.103434	0.230967	0.160148	0.143042	0.259503	0.171693	0.124786

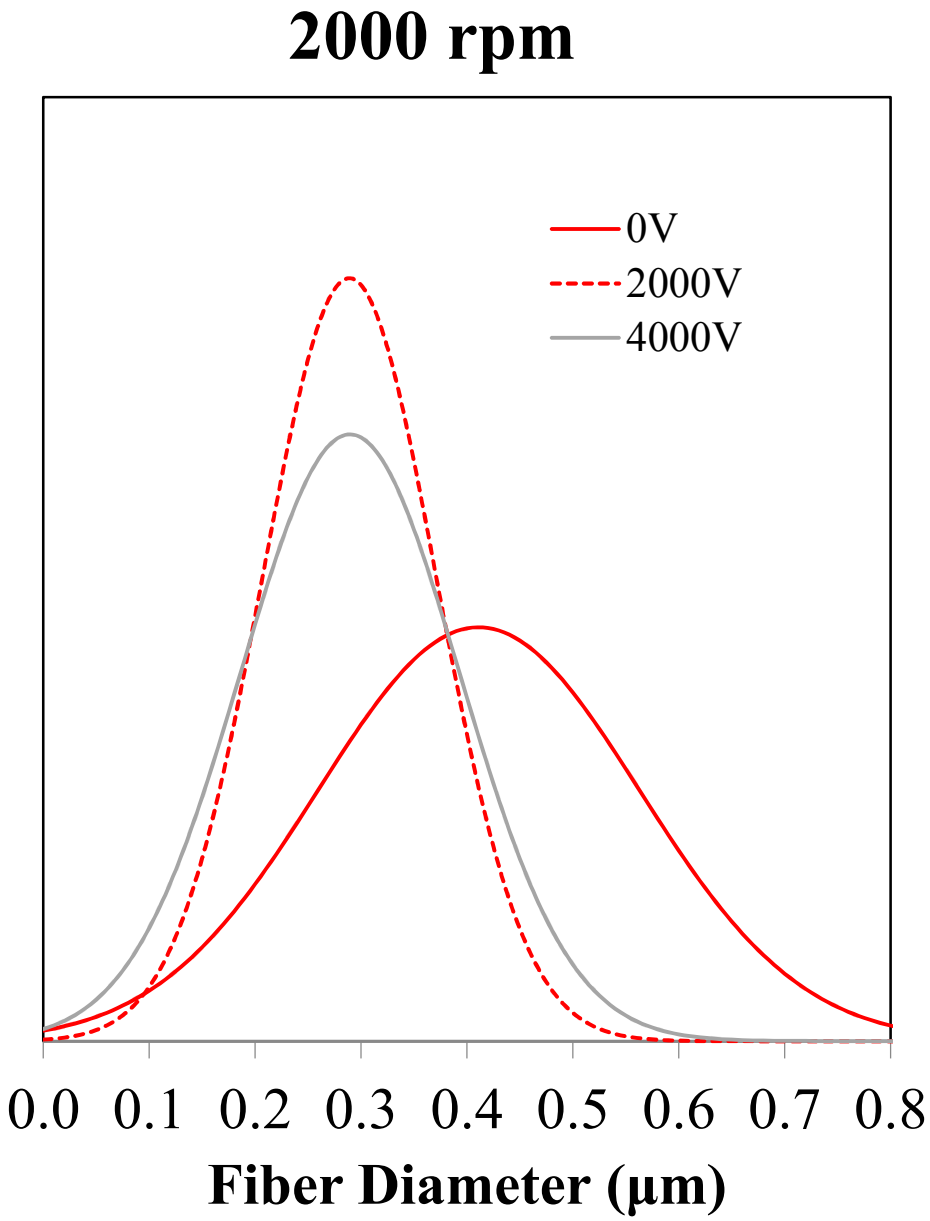

Figure 22: Normal distribution of fiber diameter measurements for 2000 rpm runs at varying input voltages.

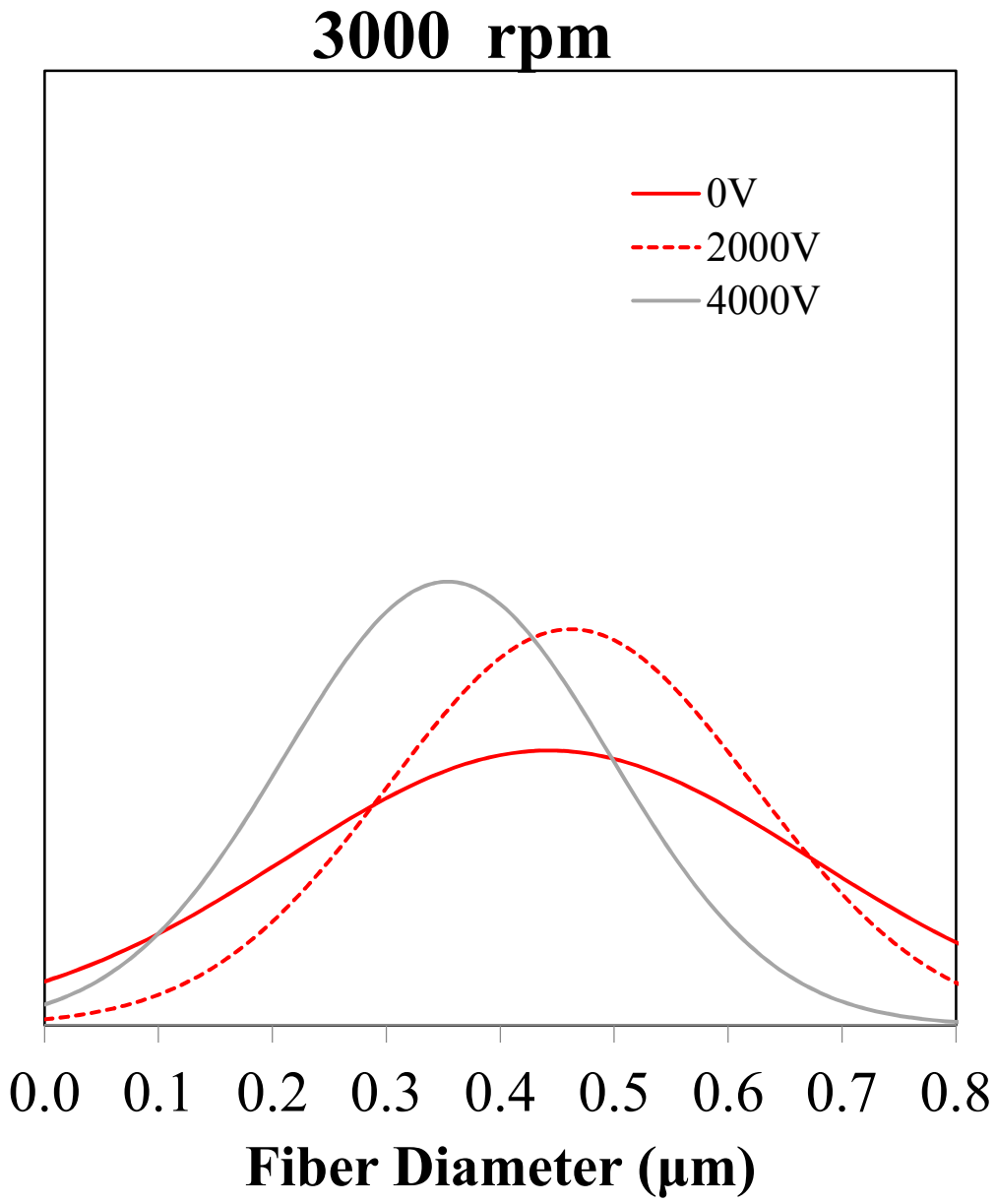

Figure 23: Normal distribution of fiber diameter measurements for 3000 rpm runs at varying input voltages.

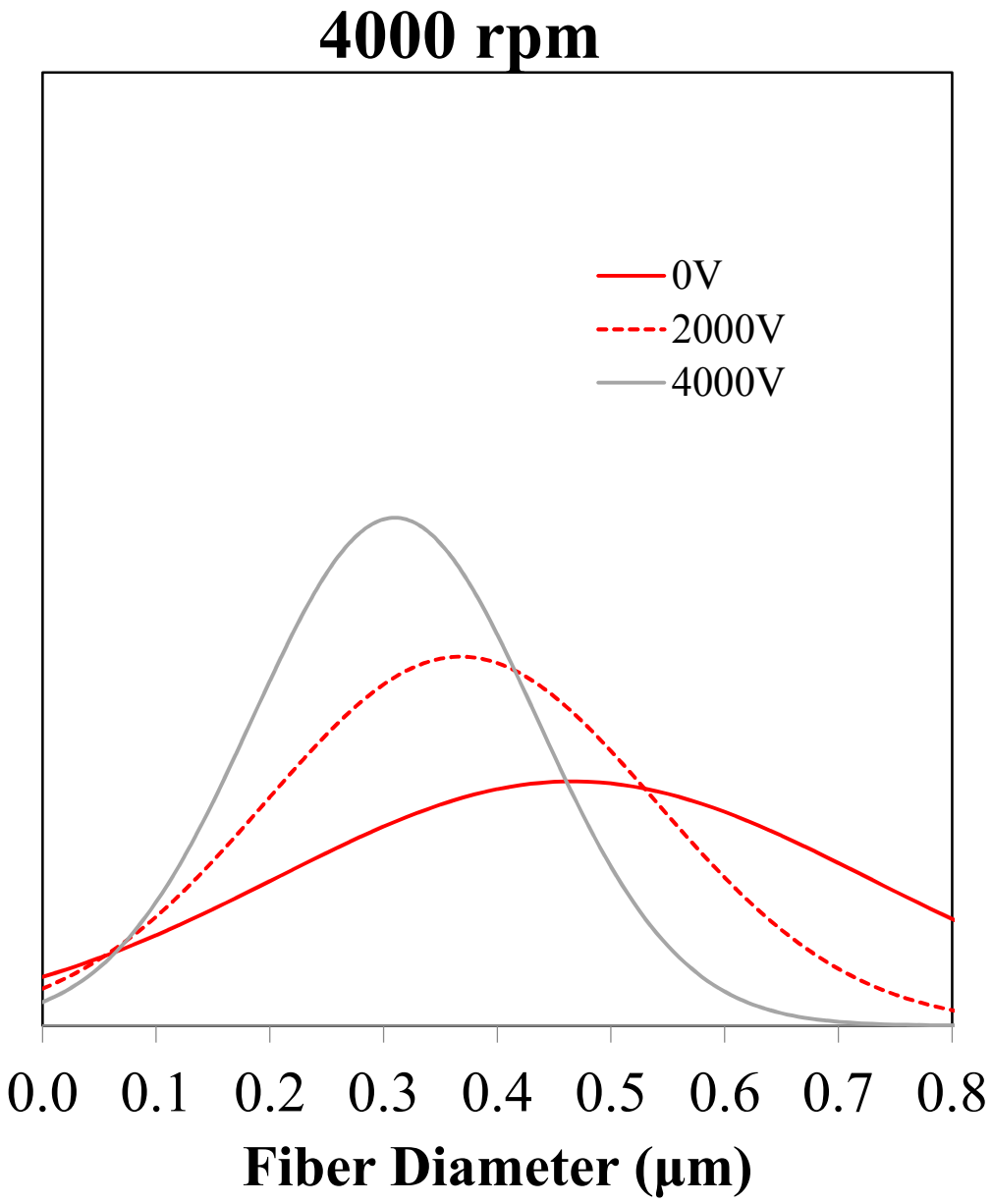

Figure 24: Normal distribution of fiber diameter measurements for 4000 rpm runs at varying input voltages.

CHAPTER VI

CONCLUSION

Electro-centrifugal spinning method for the creation of nanofibers was created and analyzed. The machine design and component interactions were carefully adjusted to mitigate any possible interference with the produced fibers. The resultant fibers displayed relations between the operating parameters, the conditions in which they were produced, and the overall quality of the fibers. Based purely on the definition of a nanofiber, the machine was not able to produce nanofibers within the range of 1 – 100 nm at the initial operating conditions for 8 wt% PEO. Following the trend of the measured fibers produced at low rotational velocity, increasing the input voltage resulted in lower fiber diameters. With some of the measured fibers being close to the 100 nm range, it may be possible to adjust operating parameters and test a solution with less viscosity to produce fibers which could be in the nanometer range.

Overall, the machine design has proven to be functional within a wide operating range. The creation of fibers for wide ranges of material systems can be done with rotational velocities between 0 – 4000 rpm without creating too many vibrations, 0 – 20,000 V potential, and needle to collector distances between 2 cm – 13 cm. Alternations to operating ranges are possible through component changes and alignment adjustments.

6.1 Future Work

Electro-centrifugal spinning is a new process being explored at UTRGV. The creation and successful testing of getting this nanofiber production method will pave the way for new fiber applications and testing procedures to be developed. While fully functional, the electro-spinning machine setup will still benefit from tests and possible upgrades that could make tunning and operating the machine a lot easier. Any improvement performed for this process should be directed towards improving the fiber quality or validating the results achieved.

One of the most important items which should be completed for the electro-centrifugal setup is to run comparison tests between the fibers it produces and those produced through the electrospinning method. Finding how this process compares with the high-quality fibers which can be achieved through electrospinning will aid in testing the validity of utilizing the electro-centrifugal spinning method.

For fibers that have been produced, special considerations should be taken for how the fibers are collected and stored. For some material systems which may benefit from a poling effect caused by the electrostatic forces in the fiber production process, following improper collection methods can cancel out the effects of poling. Although not every material system benefits from the poling byproduct from the electrostatic forces, development of a proper fiber collection process can help eliminate the chances that materials which may be affected by poling will lose those qualities.

In the research performed for the creation of this process, the testing parameters were limited to low operating conditions. Further developing the possible testing processes for the electro-centrifugal spinning machine can help broaden the understanding of how operating parameters affect the produced fibers. With the initial purpose of the electro-centrifugal spinning machine being to maintain low operating parameters, further testing should be run for keeping

low rotational velocities while increasing the voltage potentials. Following the trends that were displayed in the data of this research, it can be inferred that the produced fiber quality can further improve as the voltage goes higher.

Aside from fine-tunning operational parameters when creating fibers, maintaining good operational conditions can also improve fiber production. As was seen in the research, a slight increase in the room humidity caused the fiber yield and fiber quality to decrease. The measurements for temperature and humidity were taken from a centralized point in the room. Implementing additional sensors within the fiber production chamber can help relate the quality of the produced fibers based on external influences. Sensors that would benefit for this setup would include temperature, humidity, and vibration sensors. All of these external factors can play a significant role in the overall quantity and quality of the produced fibers.

Lastly, when fibers are being created within the electro-centrifugal spinning chamber, there is an increase in air movement within the chamber. With adjustments in design, any air that pushed the produced fibers to either the top or the bottom of the chamber were eliminated. Further testing the effects of controlled aerodynamic forces on the same plane as the fibers are being created could possible help stretch out the fibers and evaporate the solvent. A deeper look into how the aerodynamic forces would affect the produced fibers could further improve the results or add additional testing parameters for new test procedures.

REFERENCES

1. Abolhasani, M. M., Naebe, M., Hassanpour Amiri, M., Shirvanimoghaddam, K., Anwar, S., Michels, J. J., & Asadi, K. (2020). Hierarchically Structured Porous Piezoelectric Polymer Nanofibers for Energy Harvesting. Advanced Science, 7(13), 2000517. https://doi.org/10.1002/advs.202000517

2. Bandla, S., Winarski, R. P., & Hanan, J. C. (2013). Nanotomography of Polymer Nanocomposite Nanofibers. In H. Jin, C. Sciammarella, C. Furlong, & S. Yoshida (Eds.), Imaging Methods for Novel Materials and Challenging Applications, Volume 3 (pp. 193–198). Springer. https://doi.org/10.1007/978-1-4614-4235-6_26

3. Bhattacharjee, P. K., & Rutledge, G. C. (2017). 5.12 Electrospinning and Polymer Nanofibers: Process Fundamentals. In P. Ducheyne (Ed.), Comprehensive Biomaterials II (pp. 200–216). Elsevier. https://doi.org/10.1016/B978-0-08-100691-7.00165-8

4. Chaikof, E. L. (2001). Engineered collagen–PEO nanofibers and fabrics. Journal of Biomaterials Science -- Polymer Edition, 12(9), 979.

5. Dabirian, F., Hosseini Ravandi, S. A., & Pishevar, A. R. (2013). The effects of operating parameters on the fabrication of polyacrylonitrile nanofibers in electro-centrifuge spinning. Fibers and Polymers, 14(9), 1497–1504. http://dx.doi.org/10.1007/s12221-013-1497-1

6. Dabirian, F., Hosseini Ravandi, S. A., Pishevar, A. R., & Abuzade, R. A. (2011). A comparative study of jet formation and nanofiber alignment in electrospinning and electrocentrifugal spinning systems | Elsevier Enhanced Reader. Journal of Electrostatics, 69, 540–546. https://doi.org/10.1016/j.elstat.2011.07.006

7. Dahman, Y. (2017). Chapter 6—Nanopolymers**By Yaser Dahman, Kevin Deonanan, Timothy Dontsos, and Andrew Iammatteo. In Y. Dahman (Ed.), Nanotechnology and Functional Materials for Engineers (pp. 121–144). Elsevier. https://doi.org/10.1016/B978-0-323-51256-5.00006-X

8. Ding, C., Fang, H., Duan, G., Zou, Y., Chen, S., & Hou, H. (2019). Investigating the draw ratio and velocity of an electrically charged liquid jet during electrospinning. RSC Advances, 9(24), 13608–13613. https://doi.org/10.1039/C9RA02024A

9. Hosseinian, H., Valipouri, A., Ravandi, S. A. H., & Alirezazadeh, A. (2019). Determining the effect of centrifugal and electrical forces on the jet behaviors, the nanofiber structure, and morphology. Polymers for Advanced Technologies, 30(4), 941–950. https://doi.org/10.1002/pat.4528

10. Khamforoush, M., Asgari, T., Hatami, T., & Dabirian, F. (2014). The influences of collector diameter, spinneret rotational speed, voltage, and polymer concentration on the degree of nanofibers alignment generated by electrocentrifugal spinning method: Modeling and optimization by response surface methodology. Korean Journal of Chemical Engineering, 31(9), 1695–1706. https://doi.org/10.1007/s11814-014-0099-y

11. Liu, S.-L., Long, Y.-Z., Zhang, Z.-H., Zhang, H.-D., Sun, B., Zhang, J.-C., & Han, W. (2013). Assembly of Oriented Ultrafine Polymer Fibers by Centrifugal Electrospinning. Journal of Nanomaterials, 2013. https://doi.org/10.1155/2013/713275

12. Lu, Y., Li, Y., Zhang, S., Xu, G., Fu, K., Lee, H., & Zhang, X. (2013). Parameter study and characterization for polyacrylonitrile nanofibers fabricated via centrifugal spinning process. European Polymer Journal, 49(12), 3834–3845. https://doi.org/10.1016/j.eurpolymj.2013.09.017

13. Madani, M., Sharifi-Sanjani, N., Hasan-Kaviar, A., Choghazardi, M., Faridi-Majidi, R., & Hamouda, A. S. (2013). PS/TiO2 (polystyrene/titanium dioxide) composite nanofibers with higher surface-to-volume ratio prepared by electrospinning: Morphology and thermal properties. Polymer Engineering & Science, 53(11), 2407–2412. https://doi.org/10.1002/pen.23493

14. Ni, Q. Q., Jin, X. D., Xia, H., & Liu, F. (2014). 7—Electrospinning, processing and characterization of polymer-based nano-composite fibers. In D. Zhang (Ed.), Advances in Filament Yarn Spinning of Textiles and Polymers (pp. 128–148). Woodhead Publishing. https://doi.org/10.1533/9780857099174.2.128

15. Padron, S., Fuentes, A., Caruntu, D., & Lozano, K. (2013). Experimental study of nanofiber production through forcespinning. Journal of Applied Physics, 113(2), 024318. https://doi.org/10.1063/1.4769886

16. Padron, S., Patlan, R., Gutierrez, J., Santos, N., Eubanks, T., & Lozano, K. (2012). Production and characterization of hybrid BEH-PPV/PEO conjugated polymer nanofibers by forcespinning™. Journal of Applied Polymer Science, 125(5), 3610–3616. https://doi.org/10.1002/app.36420

17. Rutledge, G. C., & Fridrikh, S. V. (2007). Formation of Fibers by Electrospinning. Advanced Drug Delivery Reviews, 59, 1384–1391. https://doi.org/doi:10.1016/j.addr.2007.04.020

18. Trevino, J. E., Mohan, S., Salinas, A. E., Cueva, E., & Lozano, K. (2021). Piezoelectric properties of PVDF-conjugated polymer nanofibers. Journal of Applied Polymer Science, 138(28), 50665. https://doi.org/10.1002/app.50665

19. Weitz, R. T., Harnau, L., Rauschenbach, S., Burghard, M., & Kern, K. (2008). Polymer Nanofibers via Nozzle-Free Centrifugal Spinning. Nano Letters, 8(4), 1187–1191. https://doi.org/10.1021/nl080124q

20. Wu, T., Ding, M., Shi, C., Qiao, Y., Wang, P., Qiao, R., Wang, X., & Zhong, J. (2020). Resorbable polymer electrospun nanofibers: History, shapes and application for tissue engineering. Chinese Chemical Letters, 31(3), 617–625. https://doi.org/10.1016/j.cclet.2019.07.033

21. Yarin, A. L., Koombhongse, S., & Reneker, D. H. (2001). Taylor cone and jetting from liquid droplets in electrospinning of nanofibers. Journal of Applied Physics, 90(9), 4836–4846. https://doi.org/10.1063/1.1408260

22. Zhang, X., & Lu, Y. (2014). Centrifugal Spinning: An Alternative Approach to Fabricate Nanofibers at High Speed and Low Cost. Polymer Reviews, 54(4), 677–701. https://doi.org/10.1080/15583724.2014.935858

23. Zhang, X., Reagan, M. R., & Kaplan, D. L. (2009). Electrospun silk biomaterial scaffolds for regenerative medicine. Advanced Drug Delivery Reviews, 61(12), 988–1006. https://doi.org/10.1016/j.addr.2009.07.005

24. Zhang, Z., & Sun, J. (2017). Research on the development of the centrifugal spinning. MATEC Web of Conferences, 95, 07003. https://doi.org/10.1051/matecconf/20179507003

APPENDIX

APPENDIX

STATE OF THE ART EQUIPMENT AND SOFTWARE

State-of-the-Art-Equipment

Equipment	Purpose	Results Obtained
Rheometer	Measure the viscosity of the solution to be used for characterization	8 wt% PEO in DI H2O was very viscous and steady between $0.1s^{-1}$ and $0.5\ s^{-1}$.
SEM	Microscope to observe sub-micron fibers	Fibers created through EC spinning benefit from combining electrostatic forces and centrifugal forces as they show improvements in fiber quality and can produce at higher yields.
EC Spinning Machine	Hybrid process that combines electrospinning and centrifugal spinning to create fibers	The created fibers were in the micrometer range but adjusting operating parameters resulted in improved fiber quality which could be further researched to possibly create fibers in the nanometer scale.

State-of-the-Art Software

Equipment	Purpose	Results Obtained
ImageJ	Used to measure fiber diameter on images produced by SEM	The produced nanofibers from the EC Spinning process were measured in the micrometer range measuring between 200 nm to low micrometers.

BIOGRAPHICAL SKETCH

David Trevino was born in Hidalgo, Texas on April 23rd, 1988. He lived with his family in Pharr, Texas where he attended school in the Pharr San-Juan Alamo school district (PSJA) which includes Palmer Elementary, Pharr Elementary, Memorial Middle School, PSJA Middle School, and PSJA High School. After high school, David attended the University of Texas – Pan American briefly before withdrawing to continue to work. After years of self-development and getting married to his wife, Paula Trevino, he returned in August of 2015 to finish his undergrad degree at the newly renamed University of Texas – Rio Grande Valley. On July 16th, 2017 David and his wife Paula welcomed their newborn daughter Clarissa Ariel Trevino to this world. Just over a year later, David would graduate with his Bachelor of Science in Mechanical Engineering on December 2018.

In March 2019 David and Paula welcomed their second daughter, Vanessa Aurora Trevino to their family. Five months later in August 2019 David was awarded a Presidential Graduate Research Assistant role allowing him to return to the University of Texas – Rio Grande Valley to pursue a Master of Science in Mechanical Engineering working alongside Dr. Arturo Fuentes and Dr. Horacio Vasquez. In December of 2022 David achieved his goal. David may be reached by email at dat0327@gmail.com.